International Journal of Pharmaceutics, 65 (1990) 69–76
Elsevier

IJP 02188

The effect of size and mass on the film thickness of beads coated in fluidized bed equipment

R. Wesdyk, Y.M. Joshi, N.B. Jain, K. Morris and A. Newman

Bristol-Myers Squibb Pharmaceutical Research Institute, New Brunswick, NJ 08903 (U.S.A.)

(Received 19 February 1990)
(Accepted 23 May 1990)

Key words: Multi-particulate system; Fluid-bed coating; Segregation; Film thickness

Summary

The relationship between the film thickness on a bead, and the bead's size and mass in a polydispersed system was studied. Beads with a size distribution in the no. 14–20 mesh range were coated using Glatt fluidized bed units equipped with a Wurster insert. The coated beads were separated into narrower size fractions and dissolution testing of each fraction was performed using the USP basket method. The larger beads exhibited much slower release rates compared to the smaller beads, and the differences could not be explained by the relative surface areas. Examination of the beads by scanning electron microscope indicated that the larger or heavier beads received a thicker film compared to the smaller or lighter beads. This trend was attributed to differences in the fluidization patterns and velocities of the various sized beads.

Introduction

Modified release dosage forms are often desired for a variety of reasons, including the ability of these systems to improve patient compliance, maintain therapeutic blood levels for the duration of therapy, and reduce any drug-related side effects. A multi-particulate modified release dosage form is often preferred because the failure of a single unit of the system does not compromise the performance of the whole entity.

One of the techniques employed to manufacture such formulations involves preparation of beads by extrusion/spheronization, followed by coating with a water-insoluble polymer film. This film or coating, is used to regulate the release of drug from the core bead, and is generally applied using a fluidized bed coating system. In particular, the use of a Wurster or tangential spray mode is preferred (Mehta and Jones, 1985). Many published articles (Jones, 1985; Mehta, 1988) identify processing parameters critical to the formation of a continuous and uniform film on the substrate. It is generally recognized that such a technique yields evenly coated beads with uniform film thickness in a monodispersed system. The core (uncoated) beads, however, whether manufactured by powder or solution layering, or extrusion/spheronization techniques, are usually somewhat varied in terms of particle size and mass. While the effect of particle size and surface area differences on the film thickness of different size beads in separate monodispersed beds has been studied (Ragnarsson

Correspondence: R. Wesdyk, Bristol-Myers Squibb Pharmaceutical Research Institute, One Squibb Drive, New Brunswick, NJ 08903, U.S.A.

0378-5173/90/$03.50 © 1990 Elsevier Science Publishers B.V. (Biomedical Division)

and Johansson, 1988), the impact of particle size and mass on the characteristics of the film formed on beads in a polydispersed system has received very little attention.

In the present study, two formulations of beads, with different bulk densities, were coated in a fluidized bed apparatus equipped with a Wurster insert to investigate the effect of particle size and mass distribution on various characteristics of the coated beads.

Experimental

Methods of manufacture

For the purpose of this study, two separate core bead formulations were designed to produce beads of significantly different bulk densities. The heavier beads are designated as Formulation 1, and the lighter beads as Formulation 2. Results similar to those obtained in this study should be obtained using any beads within the same size and bulk density range.

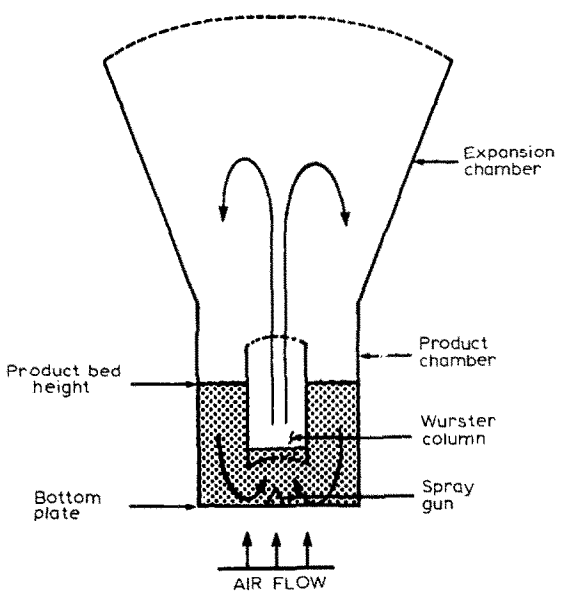

Fig. 1. Schematic diagram of fluid-bed coater equipped with a Wurster column. Approximate bed heights and particle flow patterns are also shown. Not drawn to scale.

TABLE 1

Process parameters utilized during coating

Parameter	GPCG-5	GPCG-60
Charge	5 kg	45 kg
Wurster column	9 inch	18 inch
Nozzle port	0.8 mm	1.2 mm
Partition height	3/4 inch	3/4 inch
Atomizing air pressure	2.5 bar	3.5 bar
Product temperature	40 °C	40 °C
Spray rate	7–11 g/min	40–60 g/min
Air volume	~ 60 CFM	~ 900 CFM
Curing temperature	60 °C	60 °C
Curing time	1 h	1 h
Weight gain	4.8%	4.9%

The core beads were manufactured by extrusion/spheronization, and screened to obtain a no. 14–20 mesh cut.

These beads were then coated in a Glatt coater/granulator, model GPCG-5 or GPCG-60, equipped with a Wurster column. A schematic diagram of a fluid-bed coater, equipped with a Wurster column, is given in Fig. 1. All beads from Formulation 1 were coated in the GPCG-60. The batch of beads containing a mixture of Formulations 1 and 2 was coated in the GPCG-5.

The coating was applied from aqueous polymeric systems. Typically a 4.8% w/w film level was applied. Coating process parameters are listed in Table 1.

Color coding of various sized fractions of beads was accomplished by the application of a thin film into which, FD&C Red no. 3 or FD&C Blue no. 2 dye had been incorporated.

Testing

Screening

Beads were separated into various sized fractions by sieving through appropriate U.S. Standard mesh screens.

Particle size distribution

The testing was performed on a Fritsch vibratory sieve shaker using 100 g beads at an amplitude of 4 for 3 min.

Bulk density

The testing was performed on a Sargent-Welch Volumeter. Results reported are an arithmetic mean of five measurements.

Dissolution

Dissolution testing was performed using the USP basket method. Samples of beads were filled into no. 1 hard gelatin capsule shells to yield 100 mg (drug content) potency capsules. The operating parameters are as follows: medium, 0.1 N HCl; volume, 900 ml; medium temperature, 37 °C; rpm, 100. Samples were analyzed using an HPLC method.

Scanning electron microscopy (SEM)

Film thickness measurements were obtained using an Amray model 1820T SEM system. The beads were sliced into two sections, fixed onto an aluminum stage by means of carbon paint, and sputter coated with an Au/Pd alloy to reduce charging. The mount was placed on a sample stage in the vacuum chamber of the microscope, aligned, and focused for analysis. The film thickness was measured in triplicate at positions of 3:00, 6:00 and 9:00 o'clock relative to the top of the bead where the initial cut was made. The standard deviation for values obtained from this method was typically about 2 μm.

Beads from the two formulations were separated for film thickness analysis by visual appearance and confirmed by their characteristic EDX spectra.

Fig. 2. Particle size profile of beads prepared from Formulation 1 (before coating).

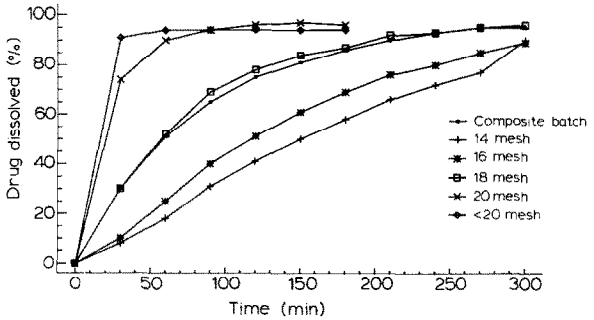

Fig. 3. Average ($n = 6$) dissolution profiles of 100 mg capsules containing various sized beads of Formulation 1 (after coating). Early time points are not shown for clarity's sake.

EDX analysis of cross-sectioned beads was also used as a qualitative tool, to monitor the extent of solubilization of core components into the film (Brown, 1986; Ghebre-Sellassie et al., 1986).

Coating efficiency

Coating efficiency was measured as the amount of film deposited (determined by weight gain, corrected for moisture loss or gain) versus the theoretical amount applied.

Results and Discussion

The size distribution profile of a batch of Formulation 1 beads is given in Fig. 2. The data indicated that there were three main fractions and smaller percentages of other sized beads. This is typical of beads manufactured by an extrusion/spheronization process. The bulk density of beads from this formulation was determined to be 0.8 g/cm^3.

These beads were coated and screened into the five narrow sized fractions which were retained on no. 14, 16, 18, 20 and < 20 mesh screens. Each fraction was separately encapsulated in no. 1 shells to yield 100 mg potency capsules. Capsules were also prepared from the composite batch (before screening; containing all size beads). Dissolution testing was performed on these capsules. The results of the dissolution testing are given in Fig. 3. These results indicate that the larger beads released drug at a much slower rate than the smaller

beads, and that the capsules from the composite batch (beads before screening) released drug at a rate consistent with a weighted fraction average of all sized beads. The trend, in which the smaller beads release drug at a faster rate than the larger beads, is not unusual. A general relationship describing the dissolution process was first observed by Noyes and Whitney (1897). The Noyes-Whitney relationship states that

$$dC/dt = K \cdot S(C_s - C) \quad (1)$$

where S represents the surface area of the beads, C_s is the concentration of a saturated solution of drug and C denotes the drug concentration at time t and

$$K = D/V \cdot h \quad (2)$$

where D denotes the diffusion coefficient of the dissolved drug, V is the volume of the dissolution media and h is the thickness of the diffusion layer.

This demonstrates that, if all other factors are held constant, the release rate is proportional to the surface area of the beads. The smaller beads have a greater surface area per unit mass than the larger beads, and will release drug at a faster rate. Therefore, while the trend was not unexpected, it was necessary to determine if surface area considerations would explain the magnitude of the differences in the dissolution profiles.

Release rates were estimated from the initial portion of the dissolution curves (Fig. 4) using standard linear regression analysis. In addition,

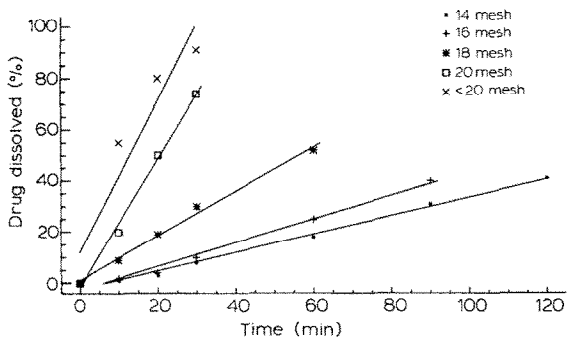

Fig. 4. Regression results of the initial portions of dissolution profiles given in Fig. 3.

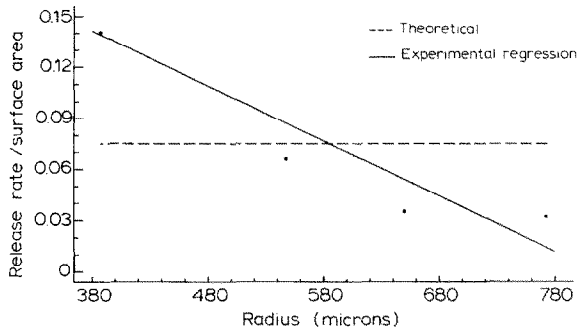

Fig. 5. Average ($n = 6$) release rates, normalized for surface area, of various sized beads from Formulation 1 (after coating).

the total bead surface area per capsule was calculated from the bead radius, as determined from the average of the upper and lower screen mesh diameter of each fraction. The results of these calculations are presented in Table 2.

Eqn 1 can be modified to normalize release rates for surface area differences. If one assumes that the film thickness is constant, the normalized release rate is independent of the size of the beads.

However, as the data presented in Fig. 5 clearly indicates, the release rate, when normalized for surface area, is dependent on the bead size. Therefore, it was apparent that the magnitude of the differences in the dissolution profiles of the various sized beads was not only a result of surface area differences but, the release rates of the beads was affected by some other parameter as well.

The film thickness of the cross-sections of beads from this batch was examined by scanning electron microscopy. Theoretically, it would be expected that various size beads dispersed in a single

TABLE 2

Surface area and release rate data for capsules containing various size fractions of beads

Average bead diameter (mm)	Total surface area per capsule (cm^2)	Release rate (% drug dissolved/min)
1.54	1.0_7	0.3_4
1.30	1.2_6	0.4_5
1.10	1.5_0	1.0_0
0.92	1.7_9	2.4_7
0.77	2.1_4	3.0_3

bed would receive an amount of film proportional to the surface area of the beads, and hence, the film thickness (amount per unit surface area) of the beads would be the same. However, it was observed that the film thickness of the various sized beads was not uniform (Fig. 6). The larger beads within the batch received a thicker coating than did the smaller beads, and therefore displayed a significantly slower dissolution rate. Although this experiment established the effect of the bead's size on the amount of film received, the effect of bead's mass could not be examined independently of size.

To investigate the effect of mass as well as size, a batch containing equal volumes of beads from Formulations 1 and 2 was coated. To accomplish this, core (uncoated) beads from both Formulations 1 and 2 were manufactured separately, and the bulk density of beads from each formulation was determined to be 0.8 and 0.6 g/cm^3, respectively. The amount of beads in the various sized fractions of each batch was adjusted so that the size distribution profiles of both batches was equivalent. The two batches were then combined in equal volume fractions and coated. After coating, the beads were screened, separated by formulation, and the film thickness measured. The results are given in Table 3. The coating efficiency, and the extent of solubilization of core components into the film was monitored to ensure that no formulation characteristic, other than differences in size or density, was contributing to differences in film thickness.

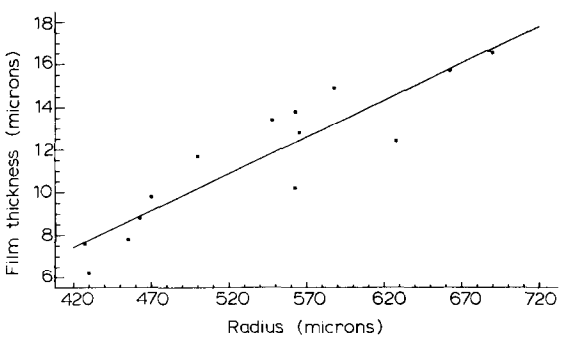

Fig. 6. Film thickness of individual beads of various sizes from Formulation 1 (after coating). Particle size determined as average radius of two particle diameter measurements by SEM.

TABLE 3

Film thickness [a] data for beads from Formulations 1 and 2

Bead size (mesh no.)	Film thickness (μm)	
	Formulation 1	Formulation 2
12–14	17.1	14.0
14–16	14.1	12.4
16–18	12.7	11.2
18–20	10.9	10.6
20–25	9.8	9.6

[a] Film thickness values reported are an average of measurements made on five particles.

Consistent with the previous batches, the data indicate that the larger beads of each formulation received a thicker film than did the smaller beads. The data further show that for each sized fraction, the heavier, or more dense beads of Formulation 1 received a thicker film than the beads of Formulation 2. Thus, it can be seen that both a bead's size and mass (or density) affected the amount of film applied to that bead when coated in this type of system.

An attempt was made to rationalize the observed trends in film thickness on the basis of fluidization patterns and velocities of the various size beads. If the beads segregated when exiting the Wurster partition, and were fluidized to different heights within the expansion chamber, the cycle times of the beads would be different. Cycle times determine the number of cycles through the coating zone. The segregation of particles to different fluidization heights has been reported previously by other workers (Bilbao et al., 1988; Daw and Frazier, 1988; Donzi and Ferrari, 1988) studying similar systems such as fluid-bed dryers. A second rationale is that the beads are fluidized to different velocities within the coating zone, or Wurster partition. The faster a bead passes through the coating zone, the less film is applied. The two hypotheses are inter-related, because the bead's velocity through the Wurster column is one factor which determines the fluidization height.

The potential for segregation of beads and different fluidization patterns was examined experimentally. Small windows in both the product and expansion chambers of the fluid bed unit allow for

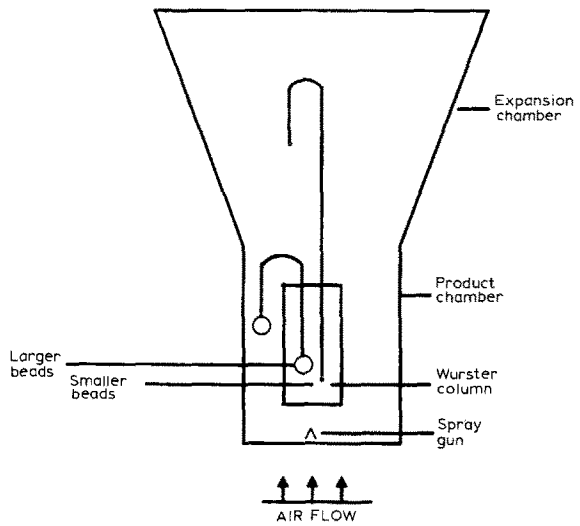

Fig. 7. Observed fluidization patterns of various sized pellets in fluid-bed coater equipped with a Wurster column. Not drawn to scale.

the observation of fluidization patterns. A means was therefore devised to observe the fluidization patterns of beads of varying size and mass. A batch of uncoated beads from Formulation 1 was screened into its various size fractions. A thin film containing blue dye was applied to the large beads (14–16 mesh), a thin film containing a red dye was applied to the small beads (20–25 mesh), and the middle size fraction (16–20 mesh) was left uncoated (white). The beads were then recombined, fluidized in the coater, and the fluidization patterns observed. The results of this experiment (Fig. 7) indicated that the smaller beads were fluidized much higher into the expansion chamber of the coater and therefore cycled fewer times per batch through the coating zone when compared to the larger beads. This was believed to be one of the reasons for the thicker films observed on the larger beads. The downbed time (time to travel from the top of the product bed to the bottom of the product chamber) did not seem to be affected by bead size as the entire product bed appeared to move as a single mass.

Bead velocities within the coating zone, or Wurster column, could not be examined experimentally. However, analysis of the forces acting on the beads as they are fluidized yields a qualitative explanation of the behavior. This analysis also indicates that there will be differences in fluidization velocities in areas other than just the Wurster column.

There are two (primary) forces acting on the beads during the fluidization process, namely, the effect of gravity, and the effect of the fluidizing air. A bead's acceleration upward, through the Wurster column, or coating zone, is a function of these two forces and can be given by,

$$a_{\text{upward}} = a_{\text{fluidizing air}} - a_{\text{gravity}} \tag{3}$$

The acceleration due to gravity is a constant and will be given by K'. The main force to be concerned with is the effect of the fluidizing air. The force of the fluidizing air on a bead is a function of the drag of that air on the particle and can be expressed as (Perry and Green, 1984),

$$F_{\text{drag}} = C \cdot p \cdot A \cdot (V)^2/2 \tag{4}$$

where C is the drag coefficient (of sphere), p corresponds to the density of surrounding fluid (air), A is the projected area of particle in the direction of motion (cross-sectional area of bead) and V denotes the relative velocity between particle and fluid (air).

In the simplest case, where V^2 is constant, this force is a function of a bead's cross-sectional area. The extent to which the drag accelerates the bead is a function of its mass (M), as given by,

$$F = M \cdot a \tag{5}$$

A bead's acceleration due to the drag is therefore expressed by

$$a_{\text{drag}} = C \cdot p \cdot A \cdot (V)^2/2M \tag{6}$$

or,

$$a_{\text{drag}} = (K) \cdot A/M \tag{7}$$

where $K = C \cdot p \cdot (V^2/2)$.

Substituting this into Eqn 3, the bead's upward acceleration is given by,

$$a_{\text{upward}} = [(K) \cdot A/M] - K' \tag{8}$$

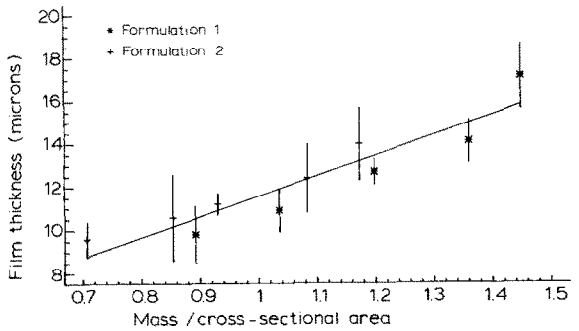

Fig. 8. Average ($n = 5$) film thickness values modelled against an average pellet's mass per unit cross-sectional area. Average mass determined from 200 pellets. Cross-sectional area calculated from median particle size of each fraction. Error bars are standard deviation of film thickness (SEM) measurements.

The bead's upward acceleration is a function of its cross-sectional area per unit mass. However, the amount of film applied to the bead is inversely proportional to the bead's velocity through the coating zone. Therefore, the amount of film applied would be a function of a bead's mass per unit cross-sectional area. A plot of film thickness against this ratio is shown in Fig. 8. The data indicates that the film thickness models well against the bead's mass/cross-sectional area ratio. The larger beads have a greater mass per unit cross-sectional area value than the smaller beads, and received a thicker film.

Due to the tapered design of the expansion chamber, the velocity of the fluidizing air gradually decreases. At a given point, the velocity of the fluidizing air is less than that which is necessary to support the bead. At this point the bead begins to accelerate in a downward direction, into the outer chamber. The beads continue to fall because the force of the fluidizing air is significantly less in the outer chamber due to the design of the bottom plate. This plate allows a greater volume of the fluidizing air to pass through the center section (Wurster column), than through the outer section.

A bead's downward acceleration is a function of the effect of gravity and the fluidizing air, and is given by,

$$a_{\text{downward}} = a_{\text{gravity}} - a_{\text{fluidizing air}} \tag{9}$$

The acceleration due to gravity is a constant and will be given by K'. The acceleration due to the fluidizing air is given in Eqn 7, and therefore, a bead's downward acceleration is expressed as

$$a_{\text{downward}} = K' - [(K) \cdot A/M] \tag{10}$$

As the smaller beads have a greater cross-sectional area per unit mass value than the larger beads, they fall more slowly into the downbed. This compounds the differences in the fluidization patterns and cycle times observed in the earlier experiment.

It is therefore believed that the differences in film thicknesses observed for the various size beads are related to differences in the beads' fluidization patterns and velocities in the coating unit. Although there are some studies reported in the literature (Yum and Eckenhoff, 1981) which model particle movements in fluid-bed coaters, this research has shown that more work is necessary to fully understand movements of particle systems of polydispersed size.

Conclusions

This investigation revealed that the size and mass distribution of beads coated in a fluidized bed apparatus equipped with a Wurster column will affect the film thickness of the various size beads. The larger and heavier beads within a batch coated by this method received a thicker film and therefore displayed a significantly slowed dissolution release rate when compared to smaller and lighter beads. These trends were attributed to the differences in the velocities and fluidization patterns of the various size beads.

A large variability in the dissolution profile of capsules can occur as a result of segregation of bulk coated beads prior to, or during encapsulation. Recently reported work (Lewis and Chariot, 1989) demonstrates the possibility of, and details the effect of demixing of beads during encapsulation. Therefore, the optimization of the manufacturing process, in order to produce beads of a narrow size distribution, is critical in minimizing the observations noted in this study.

Acknowledgements

The authors are grateful to Ms S. Bogdanowich, Ms T. Ellis and Dr J. Joseph for technical assistance. We also wish to thank Mr G. Lewen for valuable comments.

References

Bilbao, R., Lezaun, J., Menendez, M. and Abanades, J.C., Model of mixing-segregation for sand/straw mixtures in fluidized beds. *Powder Technol.*, 56 (1988) 149–155.

Brown, D.T., Semiquantitative investigation of tablet coats by electron probe microanalysis. *Drug Dev. Ind. Pharm.*, 12 (1986) 1395–1418.

Daw, C.S. and Frazier, G.C., A quantitative analysis of binary solids segregation in large particle gas-fluidized beds. *Powder Technol.*, 56 (1988) 165–177.

Donzi, G. and Ferrari, G., On the segregation mechanism of percolating fines in coarse-particle fluidized beds. *Powder Technol.*, 56 (1988) 153–158.

Ghebre-Sellassie, I., Gordon, R.H., Middleton, D.L., Nesbitt, R.U. and Fawzi, M.B., A unique application and characterization of Eudragit E 30 D film coatings in sustained release formulations. *Int. J. Pharm.*, 31 (1986) 43–54.

Jones, D.M., Factors to consider in fluid-bed processing. *Pharm. Technol.*, 9 (1985) 50–62.

Lewis, G. and Chariot, M., The effect of mixing coated and uncoated pellets on dissolution homogeneity. *AAPS Fourth Annual Meeting and Exposition*, Atlanta, October, 1989.

Mehta, A.M., Scale-up considerations in the fluid-bed process for controlled release products. *Pharm. Technol.*, 12 (1988) 46–52.

Mehta, A.M. and Jones, D.M., Coated pellets under the microscope. *Pharm. Technol.*, 9 (1985) 52–60.

Noyes, A.A. and Whitney, W.R., The rate of solution of solid substances in their own solutions. *J. Am. Chem. Soc.*, 19 (1897) 930.

Perry, R.H. and Green, D.W., *Chemical Engineers Handbook*, McGraw Hill, New York, 1984, pp. 5–63.

Ragnarsson, G. and Johansson, M.O., Coated drug cores in multiple unit preparations; influence of particle size. *Drug Dev. Ind. Pharm.*, 14 (1988) 2285–2297.

Yum, S.I. and Eckenhoff, J.B., *Development of fluidized-bed spray coating process for axisymmetrical particles. Drug Dev. Ind. Pharm.*, 7 (1981) 27–61.